Heliyon 7 (2021) e06220

Contents lists available at ScienceDirect

Heliyon

journal homepage: www.cell.com/heliyon

Research article

A green microwave method for synthesizing a more stable phthalazin-1-ol isomer as a good anticancer reagent using chemical plasma organic reactions

Sameh A. Rizk [a], Maher A. El-Hashash [a], Amr A. Youssef [c], Abdelfattah T. Elgendy [b,*]

[a] Organic Chemistry, Chemistry Department, Science Faculty, Ain-Shams University, Egypt
[b] Physics Department, Science Department, Ain-Shams University, 11566, Cairo, Egypt
[c] Mathematic Department, Science Department, Ain-Shams University, 11566, Cairo, Egypt

ARTICLE INFO

Keywords:
Efficient green microwave synthesis
Phthalazin-1(2H)-ol
Arrhenius model
DFT simulation
Anticancer HepG2
HCT-116 and MCF-7

ABSTRACTS

Conventional synthesis of the phthalazine has already allowed affording the phthalazin-1-one phthalazin-1-ol dynamic equilibrium that decreases the anticancer activity due to diminishing the concentration of the phthalazin-1-ol product. Nowadays, pure phthalazin-1-ol (**5**) can be gaining by using green microwave tools that increase the power of the phthalazine nucleus as an anticancer drug. A microscopic thermal kinetic parameter like activation energy and the pre-exponential factor of the chemical plasma organic reactions affording pure phthalazin-1-ol (5) is calculated by using DFT simulation is obtained. Then we fed these parameters into the exact Arrhenius model to evaluate the distribution of chemical equilibrium conditions for producing phthalazin-1-ol. The proposed novel models that matching between microscopic and macroscopic show that the thermal stability of the equivalent temperature of phthalazin-1-ol is more stable than phthalazinone-1-one (**4**) in case of using plasma organic effect (green microwave) at 485 K. The structures of the prepared compounds were explained by physical and spectral data like FT-IR, 1H-NMR. Moreover, the theoretical calculations of Gibbs entropy of the phase transfer confirmed the equilibrium state of phthalazin-1-ol with the experimental result is achieved. Briefly, we introduce a good study for obtaining more stable phthalazin-1-ol isomer by using a green microwave method which is considered as good anticancer reagents of phenolic group (OH) and p-propenyl-anisole precursor as anise oil analogous.

1. Introduction

Phthalazin-1-ol and its substituted derivatives in position 1 were reported to possess anticancer [1, 2, 3, 4, 5, 6, 7, 8], anticonvulsant [9], cardiotonic [10], vasorelaxant activities [11] and the canonical Gibbs entropy of residual mass is achieved. Our proposed novel dual system which merges both microscopic (DFT simulation) and macroscopic (kinetic Arrhenius Model) show that phthalazin-1-ol (**5**) is more stable than phthalzin-1-one (**4**). The results find a significant equilibrium temperature of the optimized structures of the phthalazine-1-ol inhibitors mounted on the cancer cell [12, 13, 14, 15]. Geometry optimization of phthalazine-1-ol and its derivatives inhibitors via plasma organic synthesis loaded on cancer surface via molecular dynamics process yields structures of low energies (i.e., stable structures) without loss byproduct, where the structure stability is expressed in terms of negative values of total energy Figure 1. During the simulation process, phthalazine-1-ol molecules are randomly rotated and translated around the cancer cell [16, 17, 18, 19, 20]. In our theoretical study we will use the output parameters of DFT simulation then we fed these results as input parameters in the exact analytical solution of kinetic Arrhenius model to find a reliable mechanism of chemical reaction conclusion [21, 22]. The thermal degradation of phthalazin-1-ol at heating rate $^{\circ}$K/sec are presented on Figure 2. From the TGA-curve: the first full half reaction at 404 K which is related to 50.8% mass loss of the benzylidenephthalide (**1**) outlined the thermal stability of the phthalazin-1-one (**4**) 50.9% than that approximately produced phthalazine-1-ol (**5**) 40%. This result agreed well with the phenomena of phthalazin-1-one = phthalazin-1-ol dynamic equilibrium. The thermal kinetic control of the phthalazin-1-one (**4**) is stabilized by 13 kcal/mol and so more yield formed (50.9%) more than yield of phthalazin-1-ol (**5**) be 40%. It was accompanied by endothermic

* Corresponding author.
E-mail address: abdelfattah.elgendy@sci.asu.edu.eg (A.T. Elgendy).

https://doi.org/10.1016/j.heliyon.2021.e06220
Received 10 May 2020; Received in revised form 24 November 2020; Accepted 4 February 2021

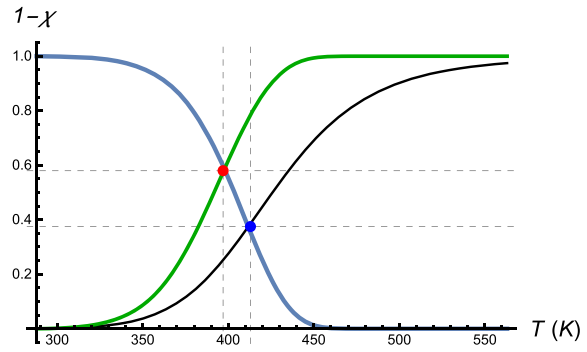

Figure 1. Physical ultrasound reaction via HOMO-LUMO of the phthalazine-1-ol inserted and overlapped to the conduction band of the cancer cell.

effect and burning via decarbonylation and decomposition of the phthalzin-1-one (**4**) that produced from the thermal degradation during the half lifetime of concentration [23, 24, 25]. In promoted microwave reaction, the thermodynamic phthalazin-1-ol (**5**) is formed at 413 K that stabilized by 36 kcal/mol due to aromaticity more than phthalazine-1-one (**4**). Therefore, our proposed novel green synthesis with dual system which combines both microscopic (DFT simulation) and macroscopic (kinetic Arrhenius Model) show that phthalazin-1-ol (**5**) is more stable than phthalzin-1-one (**4**). Based on these results we can also calculate the activation energy (E) and pre-exponential factor (A) of phthalazine-1-ol under the influence of promoted plasma organic reaction condition. Therefore, the results find a significant equilibrium temperature of the optimized structures of the phthalazine-1-ol inhibitors mounted on cancer cell [26, 27, 28].

2. Macroscopic study using theoretical Arrhenius model

In the macroscopic non-isothermal state, if an arbitrary material ensemble dissolved thermally, then the mass conversion fraction of degradable ensemble could be described in what follows [29, 30, 31, 32].

$$1-\chi_i = exp[E(T)] \tag{1}$$

Where, E(T) is dimensionless function can be calculated as:

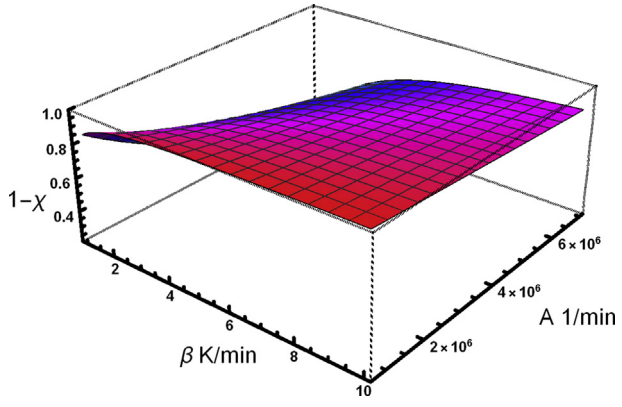

Figure 2. TGA thermal decomposing full half decomposition of benzal phthalide (3) and their capture half minimum phthalazinone production (4) [Red point; **397** K). Plasma treatment (high temperature), saving in afforded the phthalazine-1-ol (5) [Blue point; **413** K].

$$E(T) = \frac{T_0 - T}{\lambda} + \frac{\rho}{\lambda} ln\left(\frac{T}{T_0}\right) + \frac{\rho^2}{2\lambda T} F_2\left(1,1;3,2;-\frac{\rho}{T}\right) - \frac{\rho^2}{2\lambda T_0} F_2\left(1,1;3,2;-\frac{\rho}{T_0}\right) \tag{2}$$

Where, χ_i is the mass conversion fraction, 1-χ_iis the residual mass, λ = β\/A and ρ = Ei \/R, R is the gas constant. E_i is the activation energy and the constant heating rate temperature dT/dt = β. With regard to Eq. (1). The residual mass fraction of degradable ensemble represents as follow:

$$d\chi_i \Big/ dT = \frac{A\ exp[E(T)]}{\beta} exp\Big[-\frac{\rho}{T}\Big] \tag{3}$$

The equilibrium conversion of the rate constant of the Arrhenius equation can be calculated as [16]:

$$\varepsilon = \frac{kf(T)}{1 + kf(T)} \tag{4}$$

Finally, an important relationship in statistical mechanics, the entropy of canonical ensemble which is the statistical ensemble that represents the possible states of our residual mass of our system in thermal equilibrium with a heat rate of temperature can be evaluated as a canonical Gibbs entropy of residual mass like [17, 18, 19]:

$$S_{GB\chi} = -K_B(1-\chi_i)Log((1-\chi_i)) \tag{5}$$

The pervious Gibbs equation of entropy can be used to find the exact temperature of transfer phase through our chemical reaction which get the final component of chemical reaction with very low disorder of state.

3. Result and discussion

3.1. Chemistry

In chemistry, the thermodynamic stability of phthalazine-1-ol (**5**) by 36 kcal/mol is available under microwave-plasma reaction conditions due to the aromaticity and stronger of intermolecular hydrogen bond (O–H...O) than the corresponding (N–H…..O=C) of phthalazine-1-one (**4**) (Scheme 2). Sonication using polar solvent can strongly favor the amide-like structure of phthalazin-1(2H)-one tautomer (**4**) in polar protic solvent e.g. ethanol solution appears 100%, in polar aprotic solvent e.g. DMSO appears 60% [2, 3]. Otherwise, reaction in nonpolar or less polar solvent e.g. petroleum ether or acetone, it afforded the phthalazin-1-ol lactim-like structure [20, 21, 22, 33, 34, 35]. In the absence of effective solvation and at concentration less than 10^{-5} M to minimize dimeric hydrogen-bonded association, the lactam: lactim ratio is around 2:3 changing even further to 2:1 in the gas phase (Scheme 3) [23]. For first-order reactions, the pre-exponential factor (A) can fluctuate from 10^5 to 10^6 min^{-1}. In Figure 2, the residual mass decomposition of benzylidene phthalide (**1**) intersected (red point) with the final product of phthalazin-1-one **(4)** at 397 K and starting a new product of the phthalazin-1-ol (**5**) (blue point) at 413 K. The mathematical equation can indicate the typical value of the apparent activation energy(E) and pre-exponential factor(A). The Arrhenius equation is higher for the first stage of the thermal degradation of phthalazin-1-one (Table 1). The high factors are a loose complex [26, 27]. The concentrations in phthalazinone (4) are not controllable in many cases. It would have been convenient if the magnitude of the pre-exponential factor (A) showed for reaction so called molecularity. This performance is valid for non-surface-controlled reactions are having low ($<10^8$ min^{-1}) pre-exponential factors. So, the reactions of elementary can only be bimolecular. The change of entropy ΔS reflected for the activated complex configuration of the starting materials. Therefore, the formation of the phthalazine-2-ol (5) is to its thermodynamic equilibrium. Scheme 2 outlined the stronger intermolecular hydrogen bond in the phthalazine-1-ol (**5**) i.e. lower the entropy ΔS and spontaneous free energy ΔG pushing toward the phthalazine-1-ol

Table 1. Outline activation energy and Entropy of the amide-amidate rearrangement.

Compound	Activation energy (KJ)	Exponential factor A *10^6	Entropy J/mol	T_o °K	T_f °K
4	53	1.13	413	288	528
5a	60	3.3	485	295	573
5b	70	7.1	480	296	531

product. The reconstructed structure of the phalazin-1-ol using plasma process afforded a more stable isomer (5) than isomer (4) [36, 37, 38]. Using the exact model of Arrhenius model can be confirmed by the DFT simulation. Table 1 outlines that the E and A values for the thermal degradation of phthalazin1-one (4) are higher than the phthalazine-1-ol (5). The value of the activation energy E is approximately 60 kJ mol-1 that may enhance a diffusion-controlled kinetic process. For more presentation of 3D kinetic relation of variable degradation of residual mass of thermal decomposing of phthalic anhydride with phenyl acetic acid afforded benzylidene phthalide (**1**), the temperature and rate of reaction at constant heat and constant activation energy (53 k j/mole) by pre-exponential factor (1.1 10^6) Figures 3, 4, and 5. The graph shows growth rate of decomposition of mass residual of reactants **1** and **2** with increasing rate of heat constant. The thermodynamic equilibrium becomes far and yields the activated complex when reactants have higher values of activation entropy. Therefore, we can observe the short reaction times.

Also, the model shows the relation of heat constant rate and the pre-exponential factor which can give a recommendation for a good mechanism of stable reaction of phthalazin-1-ol. From our study of exact analytical solutions and the results of thermogravimetric analysis outlined in Figure 2. The addition-elimination reaction of the hydrazide (**3**) afforded the phthalazine-1-one (**4**) and phthalazine-1-ol (**5**) products at 413 K and 485 K respectively under plasma organic reaction condition (Scheme 1) (Figures 6, 7, and 8). The amide amidate of the phthalazinone-phthalazin-1-ol dynamic equilibrium occur at 432 K (orange line) (Figure 6). This shows the tautomer's unsolvated to be of approximately equal thermodynamic stability of the phthalazine-1-ol (**5**). The experimental results of the plasma organic synthesis of phthalazine-1-ol (**5**) are confirmed and good agreement with ^{1}H-NMR, theoretical and simulation studies. As seen from Figures 3, 4, 5, 6, 7, and 8.

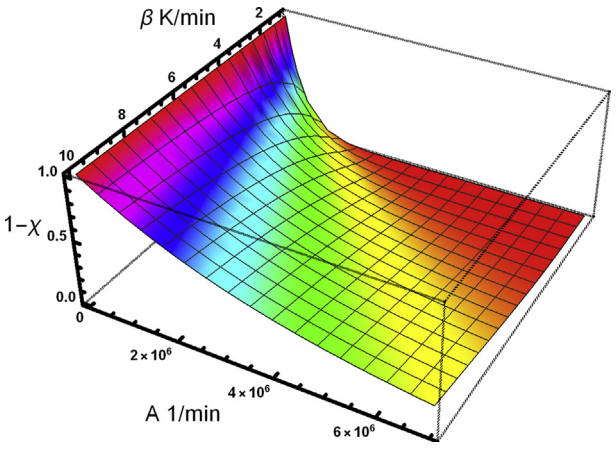

Figure 3. 3D graphical representation between the residual mass, pre-exponential factor and heat constant rate (heat control) up to (350 °K) of phthalic anhydride (**1**) and phenyl acetic acid (**2**).

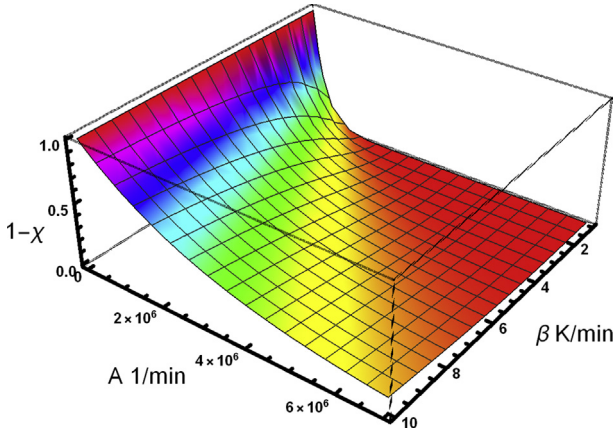

Figure 4. 3D graphical up to (397 °K) of benzykidenephthalic anhydride (**1**) and 4-chlorobenzaldehyde (**2**).

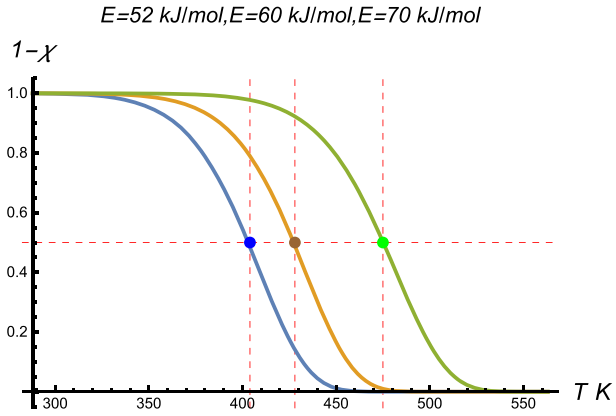

Figure 5. 3D graphical representation up to (404 °K) *5 beta* decomposing of reactants (**1**) and (**2**).

4. DFT-characterization based on the thermodynamic aspects

Phthalazin-1(2H)-one is extremely unflavored in the lactam⇌lactim dynamic in particular, the negative values of ΔS would indicate that the formation of activated complex is connected with decrease of entropy, i.e., the activated complex is "more organized" structure compared to the initial substance and such reactions are classified as "slow" [28]. From Figures 6 and 7, the authors advice that reaction takes place more effective at lower heat constant flow (β) because the higher β will decrease value of pre-exponential factor (A) which decrease the yield of the phthalazin-1-ol (**5**). The thermal stability of the phthalazin-1-ol in high energy of ultrasonic medium. The second singlet n-π* state has the lowest energy in phthalazine. In this isomer, it is the second singlet excited state, 0.46 eV above the S1 state. The S2 state in phthalazine stems from the HOMO - LUMO. DFT indicated the proposal mechanism of the phthalazine-1-ol via ring-opening of benzylidene phthalide (**1**) using

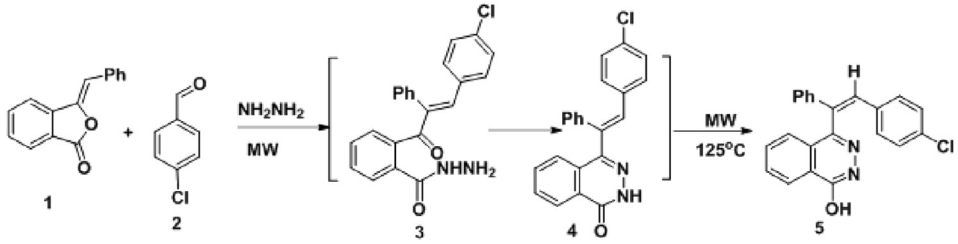

Scheme 1. Outline synthesis of the phthalazine-1-ol (5) via plasma organic reaction.

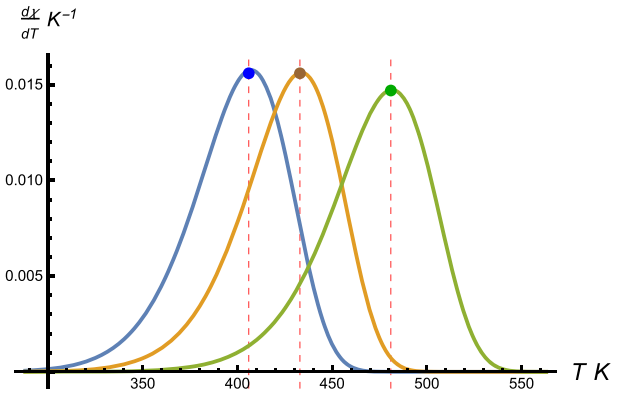

Figure 6. Decomposition of the reactants phthalazinone (4) (blue line), dynamic equilibrium (50-50) (orange line) and phthalazine-1-ol (5) (green line) by plasma temperature control.

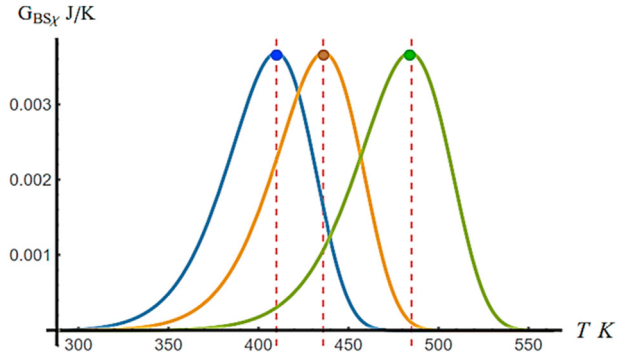

Figure 8. Outline the Gibbs entropy which indicate the phase transfer of pure phthalazinone (4) 413 K (blue line), pure phthalazine-1-ol (5) 485 K (green line) respectively under plasma treatment and dynamic equilibrium (50-50) 432 K (orange line) between the compounds **4** and **5** at plasma temperature control.

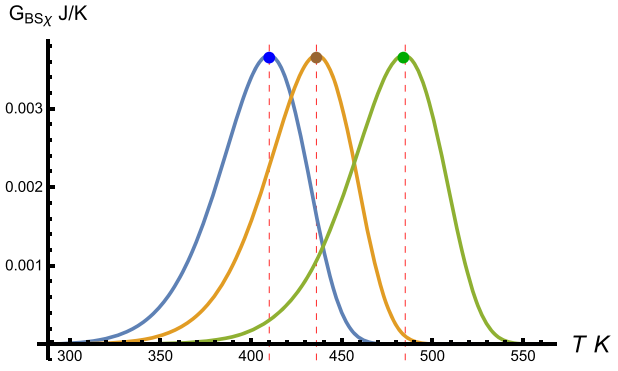

Figure 7. Outline the formation of the products of pure phthalazinone (4) (blue line), pure phthalazine-1-ol (5) (green line) and dynamic equilibrium (50-50) (orange line) between the compounds **4** and **5** at plasma temperature control.

hydrazine hydrate followed by 4-chlorobenzaldehyde (**2**) to afford the hydrazide (**3**) that is confirmed thermodynamic parameters the electrophilicity of the benzylidene phthalide was more than 4-chlorobenzaldehyde (Figure 9). Therefore, we can support the experimental suggestion [29] that the second singlet excited state of phthalazine is an np* state with a small oscillator strength. Finally, we can give also a good reason for the higher activity of phthalazin-1-ol in the cytotoxicity of anticancer due to this reaction is include the reactive speeches of OH group. The relation of equation 6 of the residual mass Gibbs entropy of the thermal degradation of the lowest disorder of the three components (benzylidene phthalide (**1**) transition phase at 410 K, phthalazine-1-one (**4**) 436 K and phthalazine-1-ol (**5**) 485 K as follow blue, yellow and Green curves respectively in Figure 8. On the other hand, the density function theory (DFT) and differential thermogravimeter DGA (Figure 7) transition phase at 406, 433 and 481 K was also confirmed the mathematical calculation in which ΔE -(E_{HO}-E_{LU}) was corresponding to the activation energy of the phthalazinone-phthalazin-1-ol dynamic equilibrium and the reaction was pushing to the phthalazin-1-ol 70% as major product. ^{1}H-NMR of the microwave product confirmed the presence of the phthalazin-1-ol (**5**) as a major product δ OH in the phthalazine-1-ol is 10.23 that higher than 6.46 ppm of the phthalazine-1(2H)-one that is approved with dihedral angle. In the phthalazine-1-ol, the dihedral angle in the structure **III** (Scheme 2) is decrease and repel with the lone pair of nitrogen of the phthalazine nucleus causing the little out of planarity and decrease the chemical shift at 3.15 ppm and 75 ppm in the ^{1}H- and ^{13}C-NMR respectively. So, in the phthalazine-1-ol (**5**), a larger dihedral angle and more planar of the benzyl moiety that agreed with the experimental ^{1}H-NMR of the microwave product appear (see more in the supplementary file). ^{1}H-NMR outline the NH appears only due to DMSO solvent is allowing for lactam lactim dynamic equilibrium and is supporting by ^{13}C-NMR that lactam form CONH is not present. ^{1}H-NMR and ^{13}C-NMR outline the dynamic equilibrium of the structures I, II and III in the DMSO solution. The lactam II-lactim I dynamic equilibrium appears in the ^{1}H-NMR in DMSO solvent and ^{13}C-NMR appears the configuration III structure (see Scheme 3).

Regioselective synthesis of 1-benzyl-4-(oxiran-2-ylmethoxy) phthalazine **6** was obtained *via* the interaction of phthalazine-1-ol **5a** with epichlorohydrin in anhydrous K_2CO_3 in dry DMF via the mechanism of nucleophilic addition, ring opening followed by ring closure through neighboring group participation devoid any band in the carbonyl region in IR spectra of the reactant **5** [30]. Moreover, synthesis of1-benzyl-4-(prop-2-yn-1-yloxy) phthalazine derivatives **7** was emanated from the reaction of phthalazine-1-ol derivatives **5** with 3-bromopropyne in the existence of K_2CO_3 anhydrous in dry acetone. Reaction of the phthalazine **7** as dipolarophile with 1,3-dipolar of phenyl azide afforded the triazole derivative **8** (Scheme 4). The dihedral angle of the phthalazine-1-ol rises the obtuse angle from 109.5° to 116.9° and 117.6°

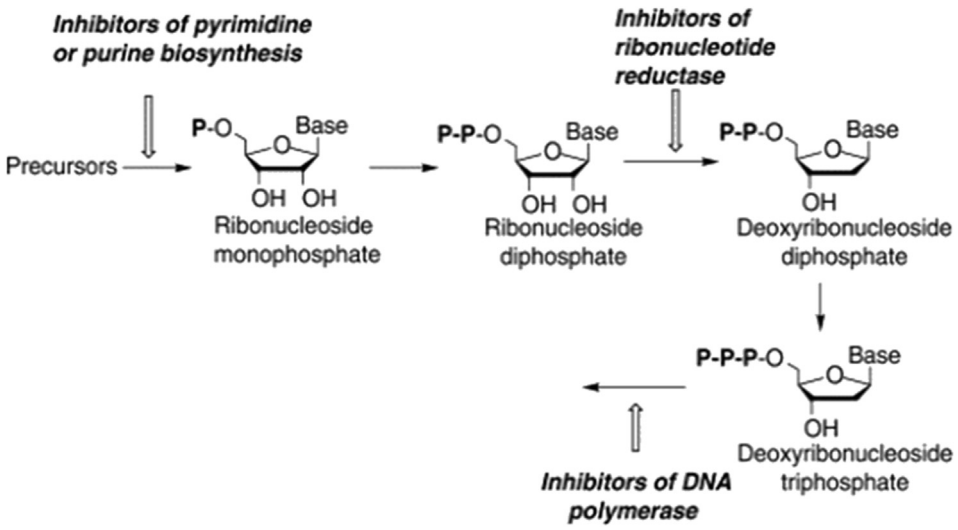

Figure 9. Outline the mechanism of drug action as inhibitor of the cancer cell.

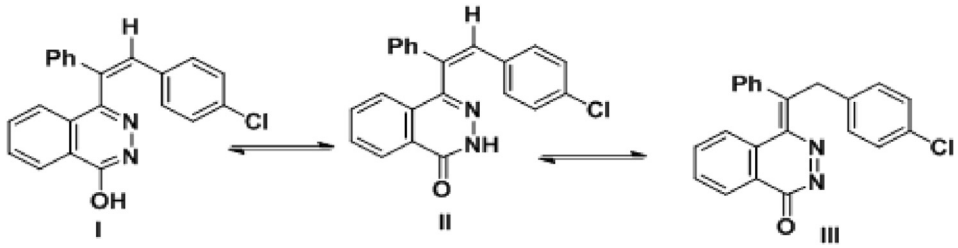

Scheme 2. Outline the stability of the phthalazine-1-ol (5) via plasma organic reaction.

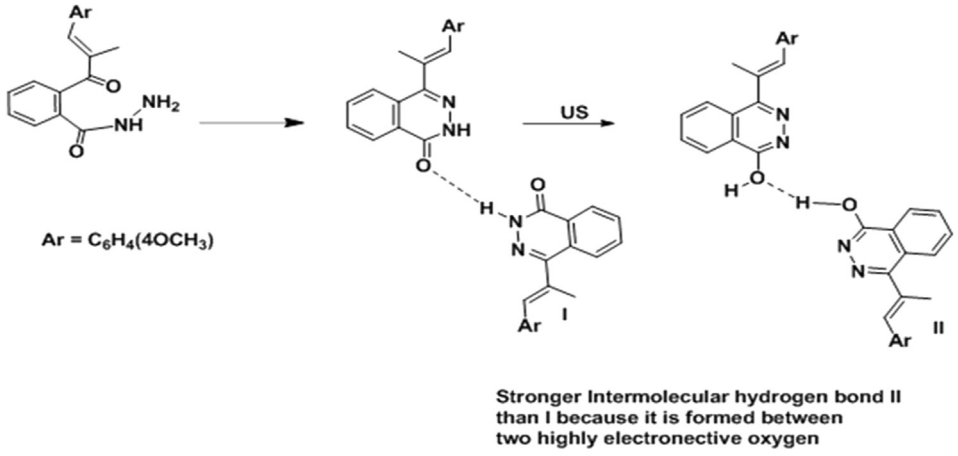

Scheme 3. Outline the stability of the phthalazine-1-ol (5) more than phthalazine-1-one (4) via intermolecular hydrogen bond.

in both of O-prop-2-ynoxy-and oxiran-2-ylmethoxyphthalazine derivatives **6** and **7** respectively can be possible deriving force to rapidity the charge transfer and become most potent for the cytotoxicity [31, 32]. Nevertheless, in the phthalazine-1)2H)-one due to dipole and Vander Waals interactions increase between the propagyl and propeneoxide precursors with the benzyl moiety lead to decrease the dihedral angle from 107.5^{o} to 104.5^{o} and 100^{o} respectively. Shrinking the dihedral angle in the phthalazinone derivatives may decrease their potential antagonist with the cancer cells due to wrapping and flatten of the phthalazine moiety.

5. Cytotoxic activity of some compounds against human tumor cells

The synthesized phthalazine-1-one (**4**), plasma-sonicated phthalazine-1-ol (**5**), Alkylated phthalazinol (**6**) and triazole derivative (**8**) compounds were tested for cytotoxic activities against three human

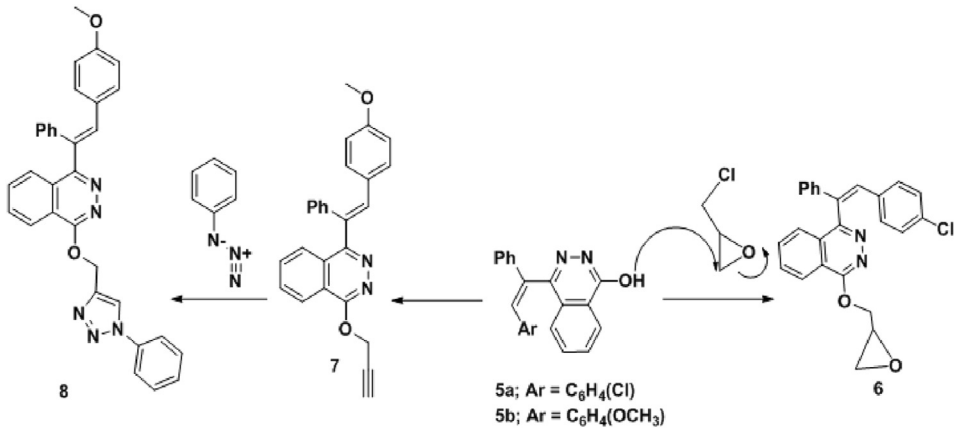

Scheme 4. Outline the synthesis of phthalazine (6,7, 8) as anticancer reagents via plasma organic reactions.

Table 2. Cytotoxic activity of phthaazin-1-ol and phthalazine-1-one compounds against human tumor cells.

Compounds	*In vitro* Cytotoxicity IC_{50} (μM)		
	HePG2	HCT-116	MCF-7
DOX	**4.50 ± 0.2**	**5.23 ± 0.3**	**4.17 ± 0.2**
5 with tautomer **4**	21.31 ± 1.8	23.90 ± 2.0	27.43 ± 2.5
Pure **5**	6.81 ± 0.1	6.16 ± 0.9	5.12 ± 0.2
6	7.23 ± 0.9	6.43 ± 0.8	7.21 ± 0.7
8	**4.43 ± 0.2**	**5.20 ± 0.2**	**4.21 ± 0.2**

IC_{50} (μM) (Half-maximal inhibitory concentration): 3–8.9 (very strong). 9–20 (strong). 21–50 (moderate). 51–100 (weak) and above 100 (non-cytotoxic); **DOX(-Doxorubicin)** = Doxorubicin. Compound **8** can be used as anticancer clinical trials in the future as DOX where Figure 9 describes the mechanism of action of the synthetic drugs 5–8 and show that the most potent is compound **8**.

tumor cells. The best results were observed for compounds phthalazine-1-ol (**5**) and their O-alkyl derivatives which found very strong cytotoxic compound. Phthalazine-1-ol **5** was considered strongly cytotoxic than phthalazine-1-one **4** which was moderate in their cytotoxic activity (Table 2). There is correlation between the cytotoxicity and the dihedral angle (C_{10}–C_{11}–C_{13}) of the benzyl substituent in the phthalazine nucleus. Effect of the dihedral angle depends on the substitution in the position 1 or 2 i.e., the presence of phthalazine-1-ol or phthalazine-1(2H)-one. The cytotoxic activity is influenced by the intermolecular hydrogen bond formation with DNA bases [39]. In addition, the positive charge on the tested synthesized compounds attracted to the negative charge on the cancer cell wall. The experimental cytotoxicity of the compounds described in this study with their structures is in good agreement. The structure-activity relationship of phthalazine 5 showed strong activity. The presence of this hardness is due to the existence of the phenolic group (OH) that may form a hydrogen bond with one of the nucleobases of the DNA and causes its damage (Figure 9). Deterioration of DNA improved via the phthalazine-OH (**5**) that facilitated the elimination reaction linking oxygen of the phosphate group at the position 3 (Figure 10) directed to single strand break of DNA molecule to prevent its repair by ligation led to inhibition of the cell cycle. So, the phthalazine-1-ol (**5**) has controlled inadequate DNA through replication leads to single-strand breaks directly caused by elimination. Moreover, the phthalazine derivative (**5**) has the same effect of DOX reference as the higher anticancer activity drug from the electronic structure (see in the Fig supplementary) that outline the HOMO and LUMO values are -2.83 and -2.60 eV respectively imitate the higher conserved thermal energy (see later in Arrhenius model) of the oxirane and triazole structures **6** and **8** as

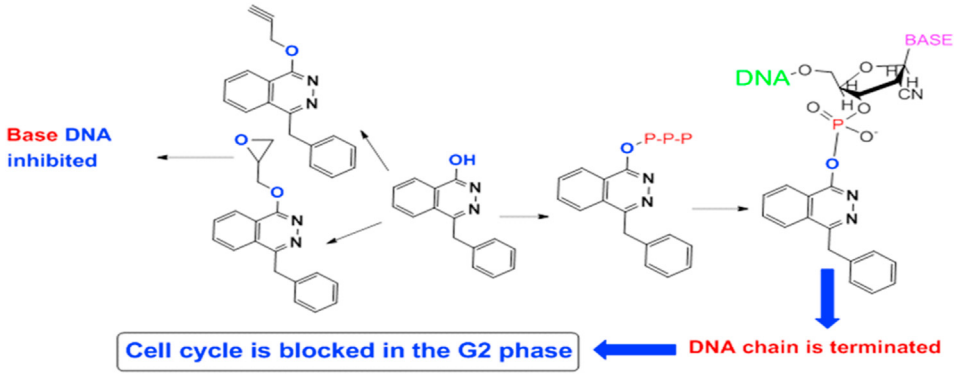

Figure 10. Outline the phthalazine-1-ol derivative as blocker the DNA carcinomic cell.

anticancer reagent. In the future research, our lab is irritating to synthesize the phthalazin-1-ol and 1-alkyl derivatives to investigate them as anticancer reagents.

6. Experimental synthesis and characterization of the organic product of phthalazine-1-ol

All melting points were measured on a Gallen Kamp electric melting point apparatus are uncorrected-The infrared spectra were recorded in potassium bromide disks on a pye-Unicam SP-3-300, Shimdazu FT IR 8101 PC infrared spectrophotometers and microwave device (6000W, Italy) at the central laboratory of faculty of science, Ain Shams University. The ^{1}H-NMR spectra were recorded on a Varian Mercury VX-300 MHz, using TMS as internal standard in deuterated dimethylsulphoxide (DMSO-d_6). Chemical shifts are measured in (δ) ppm. Sonication was performed in a Toshcon model SW 4 cleaner with a frequency of 37 KHz and operating at maximum power of 150 W. The purity of compounds was checked by TLC using silica gel (60–120) mesh as adsorbent, UV light, or iodine to accomplish visualization. All common reagents and solvents were used as obtained from commercial suppliers without further purification. The reaction flask was then placed in the maximum energy area in the microwave at the vertical tuning of flask depth displays the optimum position in which maximum surface reaction disturbance occurs. The temperature has controlled at 110–130°C, and the reaction progress was checked by TLC using CHCl3: EtOAc v/v 95:5. The reaction has continued until the starting reactants disappeared and yielded a white crystal product within 20–25 min. Once the reaction completion, the mixture was decanted into crushed ice with constant stirring, filtered, dried, and recrystallized from proper solvent.

6.1. Synthesis of 4-(Z)-4-(1-(4-chloro/methoxyphenyl) prop-1-en-2-yl) phthalazin-1-ol (5)

(Z)-3-benzylideneisobenzofuran-1(3H)-one (0.01 mol), 4-chloro- and/or 4-methoxy-benzaldehyde (0.01 mol) in the presence of potassium acetate and hydrazine hydrate (0.015 mol, 0.75mL) in ethanol (5 mL) were grinded together in a mortar with pestle were ground together in a mortar. Then, this mixture was transferred into a 250-mL round bottom flask with the addition of ethanol (5 mL). recrystallized from acetic acid. the phthalazin-1-ol **5a** Yield (93%), mp. 182–184 °C.FT-IR (KBr) (ν cm^{-1}): 3365 (OH), disappeared (CO). ^{1}H-NMR (DMSO-d_6): δ_H(ppm) 10.22 (s, 1H, OH, D_2O exchangeable), 7.7 (s, 1H, H-olifenic), 7.32–7.75 (m, 13H, ArH), 6.44 (s, 1H, NH, D_2O exchangeable). MS, m/z (%): 358 (M·+,100.0%).^{13}C-NMR (DMSO-d_6) δ 178.7, 149.7, 141.2, 132.2, 131.9, 130.1, 129.2, 128.4, 127.8, 126.4, 120.1, 39.8. *Anal.* Calc. for $C_{22}H_{15}ClN_2O$ (358): %C, 73.64; %H, 2.21; Cl, 9.88; %N, 7.81; Found: %C, 73.42; %H, 1.95; Cl, 9.71; %N, 7.54.

6.2. Synthesis of 4-(Z)-4-(1-(4-chlorophenyl) prop-1-en-2-yl)-1-methoxyoxiran-2-yl phthalazin-1-ol (6)

phthalazin-1-ol **5a** (0.01 mol), epichlorohydrin (0.01 mol) in the presence of potassium carbonate (0.015 mol, 0.75mL) in dioxane (20 mL) were refluxed together into a 250-mL round bottom flask. recrystallized from pet.ether 80–100. Yield (86%), mp. 110–112 °C.FT-IR (KBr) (ν cm^{-1}): disappeared (OH). ^{1}H-NMR (DMSO-d_6): δ_H(ppm) 8.88 (dd, 1H, Ha geminal oxirane, *J= 16.3, 5.*2 Hz), 8.63 (dd, 1H, Hb geminal oxirane, *J = 13.7, 5.*2 Hz), 7.92 (s, 1H, H-olifenic), 6.94–7.78 (m, 13H, ArH), 6.39–6.87 (dd, 1H, Hc, *J = 16.3, 13.*7 Hz). MS, m/z (%): 414 (M·+,100.0%). ^{13}C-NMR (DMSO-d_6) δ 160.7 (C), 149.7 (C), 141.2 (C), 132.2 (CH), 131.9 (C), 130.1(CH), 129.2(CH), 128.4(CH), 126.8(CH), 123.4 (CH), 118.1 (CH), 77.43 (CH), 58.33 (CH_2). *Anal.* Calc. for $C_{25}H_{19}ClN_2O_2$(414): %C, 72.37; %H, 4.62; Cl 8.54; %N, 6.75; Found: %C, 72.42; %H, 4.95; Cl 8.22; %N, 6.54.

6.3. Synthesis of 4-(Z)-4-(1-(4-chloro/methoxyphenyl) prop-1-en-2-yl)-1-methoxyprop-1-yn-2-yl phthalazin-1-ol (7)

phthalazin-1-ol derivatives **5** (0.01 mol), propagyl chloride (0.01 mol) in the presence of potassium carbonate (0.015 mol, 0.75mL) in dioxane (20 mL) were refluxed together into a 250-mL round bottom flask. recrystallized from pet.ether 80–100/benzene. Compound **7** has Yield (80%), mp. 124–126 °C.FT-IR (KBr) (ν cm^{-1}): disappeared (OH). ^{1}H-NMR (DMSO-d_6): δ_H(ppm) 8.88 (dd, 1H, Ha geminal oxirane, *J= 16.3, 5.*2 Hz), 8.63 (dd, 1H, Hb geminal oxirane, *J = 13.7, 5.*2 Hz), 7.92 (s, 1H, H-olifenic), 6.94–7.78 (m, 13H, ArH), 3.80 (s, 3H, OCH_3), 2.87 (s, 2H, CH_2), 1.67 (s, 1H, HC_{alkyne}). MS, m/z (%): 392 (M·+,100.0%). *Anal.* Calc. for $C_{26}H_{20}N_2O_2$ (392): %C, 79.57; %H, 5.14; %N, 7.14; Found: %C, 79.42; %H, 4.95; % N, 7.00.

6.4. Synthesis of 4-(Z)-4-(1-(4-chlorophenyl) prop-1-en-2-yl)-1-methoxyoxiran-2-yl phthalazin-1-ol (8)

phthalazin-1-ol **7a** (0.01 mol), phenyl azide (0.01 mol) in the presence of potassium amide (0.015 mol, 0.75mL) in ethanol (20 mL) were refluxed together into a 250-mL round bottom flask. recrystallized from acetic acid. Yield (93%), mp. 182–184 °C.FT-IR (KBr) (ν cm^{-1}): disappeared (OH), (CO). ^{1}H-NMR (DMSO-d_6): δ_H(ppm) 7.99 (s, 1H, H-olefinic), 7.18–7.97 (m, 18H, ArH), 6.11 (s, 2H, CH_2). MS, m/z (%): 514 (M·+,100.0%). *Anal.* Calc. for $C_{31}H_{22}N_5OCl$ (514): %C, 75.13; %H, 4.93; %N, 13.69; Found: %C, 75.02; %H, 4.75; %N, 13.54.

7. Conclusion

Efficient green synthesis promoted microwave via organic plasma synthesis afforded the Phthalazine-1-ol (**5**) more than phthalzin-1-one (**4**) without byproduct due to study the significant kinetic microscopic and macroscopic behavior. The study shows that (Figure 2.) the phthalazin-1-ol (**5**) has thermal equilibrium interact with lower rate of a residual mass of reaction at 485 K than the phthalazinone (**4**) at 413 K. Also, the temperature of the equilibrium state of phthalazinone (**4**) is less than the DFT (432 K). Therefore, the thermal equilibrium temperature at a lower residual mass of phthalazin-1-ol (**5**) using a green microwave is more stable. Moreover, the computed results of DFT simulation and experimental results are in good agreement with our macroscopic study of the exact Arrhenius model. In addition, to increase the rate of producing phthalazin-1-ol (**5**) we could use lower heat rate of temperature β (Figure 3.). Finally, the condition for good obtain phthalazin-1-ol (**5**) and why is exceed than phthalazinone (**4**) is achieved. The results obtained by using a plasma process can assist a better understanding of the new field of the chemical plasma organic reactions behavior behind the experiments.

Declarations

Author contribution statement

Abdelfattah T. Elgendy: Conceived and designed the experiments; Performed the experiments; Contributed reagents, materials, analysis tools or data; Wrote the paper.

Sameh A. Rizk: Conceived and designed the experiments; Analyzed and interpreted the data; Contributed reagents, materials, analysis tools or data; Wrote the paper.

Maher A. El-Hashash: Analyzed and interpreted the data; Contributed reagents, materials, analysis tools or data.

Amr A. Youssef: Performed the experiments; Contributed reagents, materials, analysis tools or data.

Funding statement

The authors gratefully acknowledge the support provided by Ain Shams Unversity, Cairo, Egypt.

Data availability statement

Data included in article/supplementary material/referenced in article.

Declaration of interests statement

The authors declare no conflict of interest.

Additional information

Supplementary content related to this article has been published online at https://doi.org/10.1016/j.heliyon.2021.e06220.

Reference

[1] C. Wang, H. Wu, T. Evron, E. Vardy, G. Han, X. Huang, S. Hufeisen, T. Mangano, D. Urban, V. Katritch, V. Cherezov, M. Caron, B. Roth, R. Stevens, Structural basis for Smoothened receptor modulation and chemoresistance to anticancer drugs, Nature commun. (2014).

[2] P.G. Tsoungas, M. Searcey, A convenient access to benzo-substituted phthalazines as potential precursors to DNA intercalators, Tetrahedron Lett. 42 (2001) 6589–6592.

[3] R. Sivakumar, S.K. Gnanasam, S. Ramachandran, J.T. Leonard, Pharmacological evaluation of some new 1-substituted-4-hydroxy-phthalazines, Eur. J. Med. Chem. 37 (2002) 793–801.

[4] Juan Li, Yan-Fang Zhao, Xiao-Ye Yuan, Jing-Xiong Xu, Ping Gong, Synthesis and anticancer activities of novel 1,4-disubstituted phthalazines, Molecules 11 (7) (2006 Jul) 574–582.

[5] S. Elmeligie, A. Aboul-Magd, D. Lasheen, T. Ibrahim, T. Abdelghany, S. Khojah, K. Abouzid, Design and synthesis of phthalazine-basedcompounds as potent anticancer agents with potential antiangiogenic activity via VEGFR-2 inhibition, J. Enzym. Inhib. Med. Chem. 34 (2019) 1347–1367.

[6] A. El-Helby, R. Ayyad, H. Sakr, K. El-Adl, M. Ali, F. Khedr, Design, synthesis, molecular docking, and anticancer activity of phthalazine derivatives as VEGFR-2 inhibitors, Arch. Pharmazie 350 (2017) 1700240.

[7] A. Turky, A. Bayoumia, A. Ghiatya, A. El-Azab, A. Abdel-Aziz, H. Abulkhaira, Design, synthesis, and antitumor activity of novel compounds based on 1,2,4-triazolophthalazine scaffold: apoptosis-inductive and PCAF-inhibitory effects, Biorg. Chem. 101 (2020) 104019.

[8] S.A. Rizk, S.S. Abdelwahab, A.A. El-Badawy, Design, regiospecific green synthesis, chemical computational analysis, and antimicrobial evaluation of novel phthalazine heterocycles, J. Heterocycl. Chem. 56 (2019) 2347–2357.

[9] N. Haider, T. Kabicher, J. Käferböck, A. Plenk, Synthesis and in-vitro antitumor activity of 1-[3-(Indol-1-yl)prop-1-yn-1-yl]phthalazines and related compounds, Molecules 12 (8) (2007) 1900–1909.

[10] S. Zhang, Y. Zhao, Y. Liu, D. Chen, W. Lan, Q. Zhao, C. Dong, L. Xia, P. Gong, Synthesis and antitumor activities of novel 1,4-disubstituted phthalazine derivatives, Eur. J. Med. Chem. 45 (8) (2010) 3504–3510.

[11] M.A. El-Hashash, S.A. Rizk, F.A. El-Bassiouny, D.B. Guirguis, S.M. Khairy, Guirguis, Facile synthesis and structural characterization of some phthalazin-1(2H)-one derivatives as antimicrobial nucleosides and reactive dye, Egypt. J. Chem. 60 (2017) 407.

[12] A.T. Elgendy, T. Abdallah, Cancer therapy system based on gold nanoparticle/cold plasma via stimulated singlet oxygen production, J. Phys.: Conf. Ser. 1253 (2019), 012003.

[13] A.T. Elgendy, A. AbdelAty, A. Youssef, M. Khder, K. Lotfy, S. Owyed, Exact solution of Arrhenius equation for non-isothermal kinetics at constant heating rate and n-th order of reaction, J. Math. Chem. (2019).

[14] A.T. Elgendy, A. Youssef, S.A. Rizk, Which energetically favorable sustainable synthesis of 4-amino-8-azacoumarin ester or 4-hydroxy-3-cyano derivative based on new exact kinetic Arrhenius and DFT stimulation, J. Iran. Chem. Soc. (2020).

[15] M. Agrawal, P. Kharkar, S. Moghe, T. Mahajan, V. Deka, C. Thakkar, A. Nair, C. Mehta, J. Bose, A. Kulkarni-Almeida, D. Bhedi, R.A. Vishwakarma, Discovery of thiazolyl-phthalazinone acetamides as potent glucose uptake activators via high-throughput screening, Bioorg. Med. Chem. Lett 23 (20) (2013) 5740–5743.

[16] M. Elagawany, M.A. Ibrahim, H.E. Ali Ahmed, A.S.H. El-Etrawy, A. Ghiaty, Z.K. Abdel-Samii, S.A. El-Feky, J. Bajorath, Design, synthesis, and molecular modelling of pyridazinone and phthalazinone derivatives as protein kinases inhibitors, Bioorg. Med. Chem. Lett 23 (7) (2013) 2007–2013.

[17] J.Y. Cho, H.C. Kwon, P.G. Williams, P.R. Jensen, W. Fenical, Azamerone, a terpenoid phthalazinone from a marine-derived bacterium related to the genus Streptomyces (Actinomycetales), Org. Lett. 8 (12) (2006) 2471–2474.

[18] E. Olmo, B. Barboza, M.I. Ybarra, J.L. López-Pérez, R. Carrón, M.A. Sevilla, C. Boselli, A. San Feliciano, Vasorelaxant activity of phthalazinones and related compounds, Bioorg. Med. Chem. Lett 16 (10) (2006) 2786–2790.

[19] S. Calligaris, L. Manzocco, L.S. Conte, M.C. Nicolia, Application of a modified Arrhenius equation for the evaluation of oxidation rate of sunflower oil at subzero temperatures, J. Food Sci. 69 (8) (2004) 361–366.

[20] M. Schwaab, J.C. Pinto, Optimum reference temperature for reparameterization of the Arrhenius equation. Part 1: problems involving one kinetic constant, Chem. Eng. Sci. 62 (2007) 2750–2764.

[21] J.A. Pearce, Relationship between Arrhenius models of thermal damage and the CEM 43 thermal dose, SPIE BiOS: Biomedical Optics 15 (2009) 718104–718114.

[22] X. He, S. Bhowmick, J.C. Bischof, Thermal therapy in urologic systems: a comparison of Arrhenius and thermal isoeffective dose models in predicting hyperthermic injury, J. Biomech. Eng. 131 (2009), 074507.

[23] A. Yelon, B. Movaghar, Microscopic explanation of the compensation (Meyer-Neldel) rule, Phys. Rev. Lett. 65 (1990) 618–620.

[24] R.R. Krug, W.G. Hunter, R.A. Grieger, Enthalpy-entropy compensation. 2. Separation of the chemical from the statistical effect, J. Phys. Chem. 80 (1976) 2341–2351.

[25] A. Yelon, B. Movaghar, R. Crandall, Multi-excitation entropy: its role in thermodynamics and kinetics, Rep. Prog. Phys. 69 (2006) 1145–1194.

[26] P.J. Barrie, The mathematical origins of the kinetic compensation effect: 2. the effect of systematic errors, Phys. Chem. Chem. Phys. 14 (2012) 327–336.

[27] P.J. Barrie, The mathematical origins of the kinetic compensation effect: 1. the effect of random experimental errors, Phys. Chem. Chem. Phys. 14 (2012) 318–326.

[28] M. Napoletano, G. Norcini, F. Pellacini, G. Morazzoni, P. Ferlenga, Pradella L. Phthalazine PDE4 inhibitiors, Part 2: the synthesis and biological evolution of 6-methoxy-1,4-disubstituted derivatives, Bioorg. Med. Chem. Lett 11 (2001) 33–37.

[29] S.A. Rizk, S.S. Abdelwahab, E. Elrazaz, Synthesis and QSAR study of some novel heterocyclic derivatives as in vitro cytotoxic agents, J. Heterocycl. Chem. 56 (2019) 443.

[30] Y.K. Ramtohup, M.N.G. James, J.C. Vederas, Synthesis and evaluation of keto-glutamine analogues as inhibitors of hepatitis A virus 3C proteinase, J. Org. Chem. 67 (2002) 3169.

[31] R. Gordillo, T. Dudding, C.D. Anderson, K.N. Houk, Hydrogen bonding catalysis operates by charge stabilization in highly polar Diels−Alder reactions, Org. Lett. 9 (2007) 501–503.

[32] H. Kissinger, Variation of peak temperature with heating rate in differential thermal analysis, J. Res. Natl. Bur. Stand. 57 (1956) 217–221.

[33] G. Marin, G.S. Yablonsky, Kinetics of Chemical Reactions: Decoding Complexity, Wiley-VCH Verlag, Weinheim, 2011.

[34] Ida E. Akerblom, Dickson O. Ojwang, Jekabs Grins, Gunnar Svensson, A thermogravimetric study of thermal dehydration of copper hexacyanoferrate by means of model-free kinetic analysis, J. Therm. Anal. Calorim. 129 (2017) 721–731.

[35] Chung-Wei Huang, Teng-Chun Yang, Ke-Chang Hung, Xu Jin-Wei, Jyh-Horng Wu, The effect of maleated polypropylene on the non-isothermal crystallization kinetics of wood fiber-reinforced polypropylene composites, Polymers 10 (4) (2018) 382.

[36] S.K. Attia, A.T. Elgendy, S.A. Rizk, Efficient green synthesis of antioxidant azacoumarin dye bearing spiro-pyrrolidine for enhancing electro-optical properties of perovskite solar cells, J. Mol. Struct. 1184 (2019) 583–592.

[37] M.A. El-Hashash, K.M. Darwish, S.A. Rizk, F.A. El-Bassiouny, The uses of 2-ethoxy-(4H)-3,1-benzoxazin-4-one in the synthesis of some quinazolinone derivatives of antimicrobial activity, Pharmaceuticals 4 (2011) 1032–1051.

[38] M.E. Azab, S.A. Rizk, N.F. Mahmoud, Facile synthesis, characterization, and antimicrobial evaluation of novel heterocycles, schiff bases, and N-nucleosides bearing phthalazine moiety, Chem. Pharm. Bull. 64 (2016) 439–450.

[39] A.M. Lord, M.F. Mahon, M.D. Lloyd, M.D. Threadgill, Design, synthesis, and evaluation in vitro of quinoline-8-carboxamides, a new class of poly(adenosine-diphosphate-ribose) polymerase-1 (PARP-1) inhibitor, J. Med. Chem. 52 (3) (2009) 868–877.